Research Article J. Electrochem. Sci. Technol., **2018**, 9(2), 157-162

Journal of Electrochemical Science and Technology
jecst.org

Herbaceous Biomass Waste-Derived Activated Carbons for Supercapacitors

Joah Han[1,2], Jin Hyung Lee[1], and Kwang Chul Roh[1,*]

[1]*Center of Energy Storage Materials, Korea Institute of Ceramic Engineering & Technology, Jinju-si 52851, Republic of Korea*
[2]*Department of Materials Science and Engineering, Korea University, Seoul 02841, Republic of Korea*

ABSTRACT

In the study, herbaceous biomass waste including giant miscanthus, corn stalk, and wheat stalk were used to prepare commercially valuable activated carbons by KOH activation. The waste biomass predominantly consists of cellulose/hemicellulose and lignin, in which decomposition after carbonization and activation contributed to commercially valuable specific surface areas (>2000 m^2/g) and specific capacitances (>120 F/g) that exceeded those of commercial activated carbon. The significant electrochemical performance of the herbaceous biomass-derived activated carbons indicated the feasibility of utilizing waste biomass to fabricate energy storage materials. Furthermore, with respect to both economic and environmental perspectives, it is advantageous to obtain activated carbon from herbaceous biomass waste given the ease of handling biomass and the low production cost of activated carbon.

Keywords : Herbaceous biomass, Biomass waste, Activated carbon, Energy storage material, Supercapacitor

Received : 30 March 2018, Accepted : 13 April 2018

1. Introduction

The utilization of herbaceous biomass is increasing around the world. In Egypt and China, a few million tons of rice straw and wheat straw are burned annually by wildfires or by the domestic burning of post-harvest as an energy source for heating [1,2]. However, this results in serious air pollution that contributes to global climate change. Thus, the aforementioned herbaceous biomasses are utilized in other fields as value-added products, including biofuels, livestock, and paper. Additionally, they are used in energy-storage materials and as absorbents for fluorine and CO_2 gas [3,4].

Supercapacitors have attracted research attention owing to the increase in electrical energy consumption in various fields ranging from large to small scale devices such as electric vehicles, portable devices, and smart phones, and this demonstrates that the electrical energy storage devices require high energy and power densities. Thus, extant studies have widely focused on supercapacitors with satisfactory performance including high power density and long cycle stability [5-7]. They are utilized in various fields such as energy back-up systems, regenerative braking systems, acceleration in hybrid vehicles, and portable devices that also require energy and power densities. However, supercapacitors have the disadvantage of low energy density. Thus, electrode active materials with high specific surface area (SSA) are used to achieve a satisfactory energy density. The electrodes are mostly constructed using carbonaceous materials, and include activated carbons, carbon nanotubes (CNTs), aerogels, template carbons, and graphene [8,9].

Waste biomass is a cheap and renewable source to prepare energy storage materials. It is predominantly composed of cellulose/hemicellulose and lignin; and these representative components can yield materials with porous structures through decomposition after carbonization and activation. In the study, abundant

*E-mail address: rkc@kicet.re.kr

DOI: https://doi.org/10.5229/JECST.2018.9.2.157

agricultural wastes, including giant miscanthus, corn stalk, and wheat stalk were used to prepare commercially valuable activated carbons by KOH activation. Specifically, KOH activation is an efficient method to fabricate microporous carbon materials with high specific surface areas, and this contributes to high specific capacitances of energy-storage materials. Thus, commercially valuable activated carbons with effective electrochemical performances can be prepared by using waste biomass.

2. Experimental

Giant miscanthus (supplied by National Institute of Crop Science, Republic of Korea), corn stalk, and wheat stalk (supplied by CJ CheilJedang Corporation, Republic of Korea, and harvested from Shansong, China) were used as the precursors of activated carbons. First, the carbonization process was performed at 800°C for 1 h under an inert atmosphere (N_2 gas) with a gas flow rate of 300 cm^3/min and heating rate of 3°C/min. Twenty grams of the individual samples were prepared for carbonization. The different biomass-derived carbons were individually mixed with KOH pellets (Sigma-Aldrich Co. LLC., Korea) by using an electric blender (the ratio of C/KOH is 25% w/w, carbon: 5 g, KOH pellet: 20 g), and the mixture was heated in a nickel vertical-type furnace at 900°C at a heating rate of 2°C/min for 1 h under an inert atmosphere (Ar gas) with a gas flow rate of 300 cm^3/min. The resultant powder was cooled to 25°C and then washed with 0.1 M HCl solution and deionized water to adjust the pH to 7. Finally, different biomass-derived activated carbons were obtained after filtration and drying at 80°C for 16 h. The obtained samples were denoted as "GMDAC" for giant miscanthus-derived activated carbon, "CSDAC" for corn stalk-derived activated carbon, and "WSDAC" for wheat stalk-derived activated carbon.

The surface morphologies of the different activated carbons were observed by field emission scanning electron microscopy, FE-SEM (JEOL, JSM-6700F, Japan). The constant mass loss of the samples was analyzed following carbonization by thermogravimetric analysis (TGA; Netzsch, Germany). In order to analyze the crystalline nature of the samples, X-ray diffraction (XRD; Rigaku D/Max 2500/PC, Japan) was performed at 40 kV and 200 mA with Cu K_α radiation (λ = 0.154 nm). The adsorption capacity and pore structure of the different activated carbons were examined by using a gas analyzer (Belsorp-Mini II, BEL, Japan). In order to estimate the electrochemical performance, rubber-type electrodes were prepared by using different biomass-derived activated carbons as the active material, polytetrafluoroethylene (Daikin Industries, Japan) as the binder, and Super P (Imerys Graphite & Carbon, Belgium) as the conductive agent, mixed in a ratio of 90:5:5 (w/w/w %). The single electrode mass and density of the GSDAC electrode were 0.011 g and 0.48 g/cc, those of the CSDAC electrode were 0.009 g and 0.41 g/cc, and those of the WSDAC electrode were 0.009 g and 0.40 g/cc, respectively. The different biomass-derived activated carbon electrodes were used as the working electrodes, and tetraethylammonium tetrafluoroborate in acetonitrile (1 M $TEABF_4$ in ACN) was used as the electrolyte to fabricate CR2032 coin cells. Additionally, the capacitive behaviors of the different activated carbons were determined by (Cyclic voltammetry, CV) using a VSP potentiostat (Biologic, France). CV was performed in the voltage range 0 V to 2.7 V at various scan rates. In this study, charge-discharge tests were performed by using a tester (Hi-EDLC-16CH, Human Instrument Co., Korea) at various current densities. Further, the cycle properties were evaluated for 2200 cycles at 5 mA/cm^2. The gravimetric specific capacitance (C_{sp}) was calculated as follows:

$$C_{sp} = \frac{2 \cdot I \cdot \Delta t}{m \cdot \Delta V} \quad (1)$$

Here, C_{sp} denotes the gravimetric specific capacitance (F/g), I the discharge current (A), Δt and ΔV the time (s) and potential window (V), respectively, and m the mass of a single electrode (g).

3. Results and Discussion

Fig. 1 shows the FE-SEM images of the surface morphologies of the samples, and Figures 1(a), (b), and (c) show the smooth surfaces of the raw materials. Figures (d), (e), and (f) show the rough surfaces of the activated carbon samples after carbonization and alkali activation. After carbonization at 800°C and KOH activation at 900°C, the samples were split, since the components of the samples were decomposed, as shown in Figs. 1 (d)-(f).

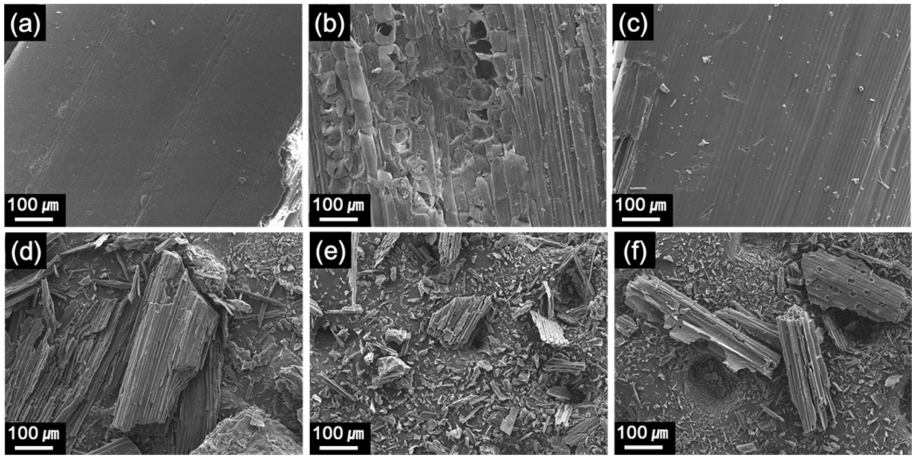

Fig. 1. FE-SEM images of (a) giant miscanthus, (b) corn stalk, and (c) wheat stalk raw materials, and (d) GMDAC, (e) CSMDAC, and (f) WSDAC formed by carbonization at 800°C and KOH activation at 900°C in an inert atmosphere.

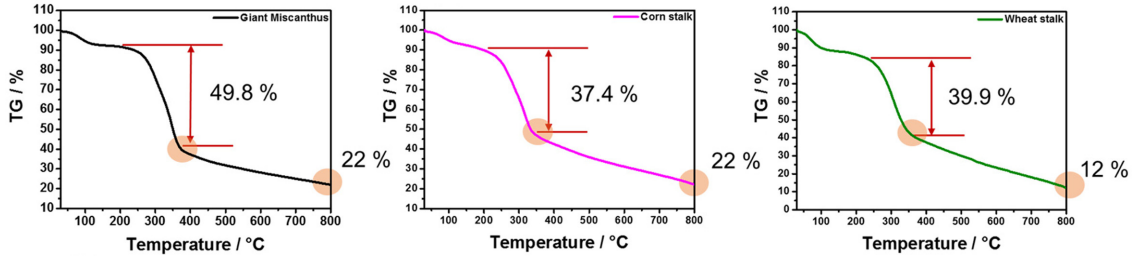

Fig. 2. Thermogravimetric profiles of raw materials heated from 30 to 800°C at a heating rate of 3°C/min under N_2 flow.

The TGA profiles in Fig. 2 show mass losses of 49.8%, 37.4%, and 39.9% at temperatures between 250°C and 400°C due to volatilization and decomposition of the inorganic or organic compounds in giant miscanthus, corn stalk, and wheat stalk, respectively [10]. The residual weights of the final products were 22%, 22%, and 12% for the giant miscanthus, corn stalk, and wheat stalk, respectively. Giant miscanthus and corn stalk exhibited the same residual weight, while wheat stalk revealed the lowest weight ratio of the final product. This is potentially due to the different contents of cellulose, hemicellulose, and lignin in the raw materials that contribute to the decomposition of the samples during carbonization. There is little difference (of approximately 10 wt.%) in the carbon yields of the herbaceous biomass and woody biomass, since herbaceous biomass exhibits a relatively lower lignin content (above 60 wt.% carbon) compared to that of the woody biomass. Therefore, the amount of carbon produced by the herbaceous biomass is slightly lower (approximately 5%) compared to that produced by the woody biomass after carbonization.

Fig. 3 shows the wide XRD patterns of the samples, revealing the (002) and (100) peaks at 26° and 43°, respectively. The (002) peaks for all the samples were broad and shifted to low angles, which implied that all the samples had a large d-spacing that is representative of an amorphous structure.

The pore structures of the activated carbons were investigated by N_2 adsorption-desorption experiments. Fig. 4 (a) reveals a type I adsorption isotherm for all the samples, thereby indicating the presence of micropores, as designated by IUPAC. However, in the case of CSDAC and commercial AC, a type IV adsorption isotherm that indicates the presence of mesopores was additionally observed [11,12].

The results indicate that the bimodal pore structure leads to both high adsorption due to the micropores and fast kinetics due to the mesopores in the superca-

pacitors. Table 1 shows the BET specific surface areas (SSA_{BET}) and pore volumes of the activated carbons. The SSA_{BET} of CSDAC is the highest (2434 m^2/g), and is attributed to the highest specific capacitance (127 F/g), as shown in Table 2. Additionally, with respect to GMDAC, CSDAC, WSDAC, and commercial AC, the total pore volumes calculated at $P/P_0 = 0.99$ are 0.99, 1.22, 1.10, and 0.82 cm^3/g, the micropore volumes calculated at $P/P_0 = 0.1$ are 0.79, 0.91, 0.86, and 0.65 cm^3/g, the mesopore volumes calculated by the Barrett-Joyner-Halenda (BJH) method are 0.14, 0.23, 0.18, and

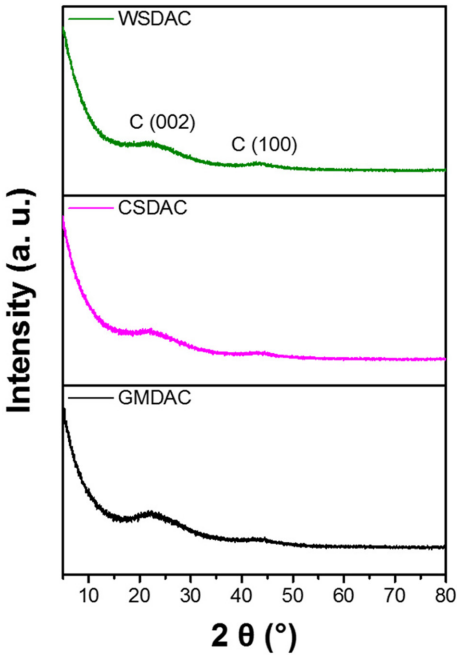

Fig. 3. Wide-angle XRD patterns of GMDAC, CSDAC, and WSDAC with the (002) peak, indicating an amorphous structure.

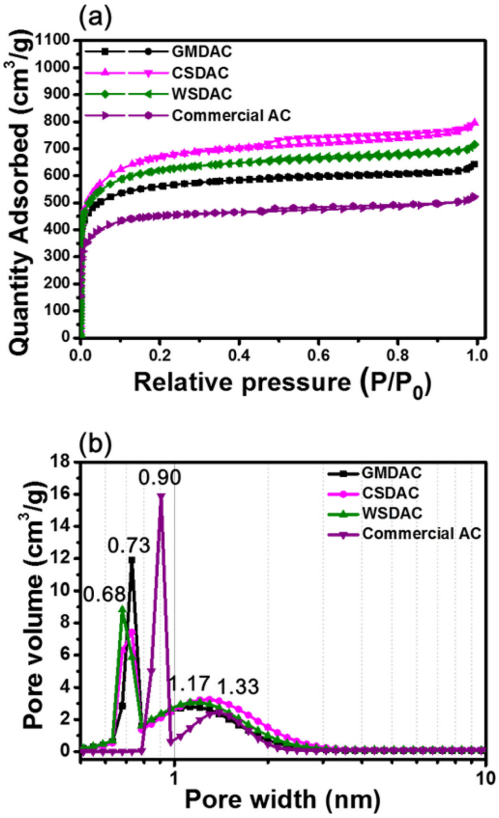

Fig. 4. (a) N_2 adsorption-desorption isotherms and (b) pore size distribution (PSD) determined from the NLDFT models of GMDAC, CSDAC, WSDAC, and commercial AC.

Table 1. Surface areas and pore structures of GMDAC, CSDAC, WSDAC, and commercial AC.

Sample	SSA_{BET} (m^2/g)	V_{total} (cm^3/g)	V_{micro} (cm^3/g)	V_{meso} (cm^3/g)	V_{macro} (cm^3/g)
GMDAC	2212	0.99	0.79 (80%)	0.14 (14%)	0.06 (6%)
CSDAC	2434	1.22	0.91 (75%)	0.23 (19%)	0.08 (6%)
WSDAC	2327	1.10	0.86 (78%)	0.18 (16%)	0.06 (6%)
Commercial AC	1732	0.82	0.65 (79%)	0.17 (21%)	-

*SSA_{BET}: Specific surface area by BET method,
*V_{total}: total pore volume, V_{micro}: micropore volume, V_{meso}: mesopore volume, V_{macro}: macropore volume

Table 2. Electrochemical data of the synthesized and commercial AC.

Activated carbons	Electrode density (g/cc)	Charge voltage (V)	Discharge voltage (V)	Gravimetric C_{sp} (F/g)		Volumetric C_{sp} (F/cc)		Capacitance retention ratio (%)
				At 0.5 mA/cm^2	At 30 mA/cm^2	At 0.5 mA/cm^2	At 30 mA/cm^2	
GMDAC	0.48	2.7	1	121	110	58	53	91
CSDAC	0.41			127	116	52	48	92
WSDAC	0.40			125	111	50	44	88
Commercial AC	0.58			100	83	58	48	83

*C_{sp}: specific capacitance

0.17 cm^3/g, and the macropore volumes are 0.06, 0.08, and 0.06, respectively, as shown in Table 1. The highest porosity and bimodal pore structure of CSDAC provide facile pathways for the electrolyte ions during charging and discharging. As shown in Fig. 4 (b), all the samples predominantly exhibit micropores with diameters below 1.3 nm, as estimated by NL-DFT. Micropores smaller than that of the solvated ions (micropore diameter below 1 nm) could improve the energy density [13,14]. In $TEABF_4$, the diameters of the solvated ions are 1.2 nm and 1.04 nm, while the diameters of the bare ions are 0.68 nm and 0.48 nm for TEA^+ and BF_4^-, respectively. It should be noted that active materials with high pore volumes and narrow pores are more beneficial for supercapacitors, since they lead to high energy and power densities [13,15]. However, micropores with diameters below 0.7 nm prevent ion diffusion [16]. The ion-sieving effect decreases the specific capacitance and rate capability. As shown in Fig. 4 (b), the pore diameters are predominantly 0.73 nm in GMDAC, 0.73 nm in CSDAC, 0.90 nm in WSDAC, and 0.68 nm in WSDAC. Thus, in CSDAC, the micropores with diameters of 0.73 and 1.33 nm are the most accessible to the electrolyte ions, which can improve the electrochemical performance of supercapacitors [17].

Figs. 5 (a) and (b) show the gravimetric and volumetric specific capacitances, respectively, of GMDAC, CSDAC, WSDAC, and commercial AC at various current densities. As shown in Table 2, the gravimetric specific capacitance (above 120 F/g) and capacitance retention ratio (above 88%) of all the synthesized activated carbons are higher than those of commercial AC. CSDAC exhibits the highest gravimetric specific capacitance and capacitance retention ratio (92%), and this is attributed to its pore structure; it also exhibits the largest specific surface

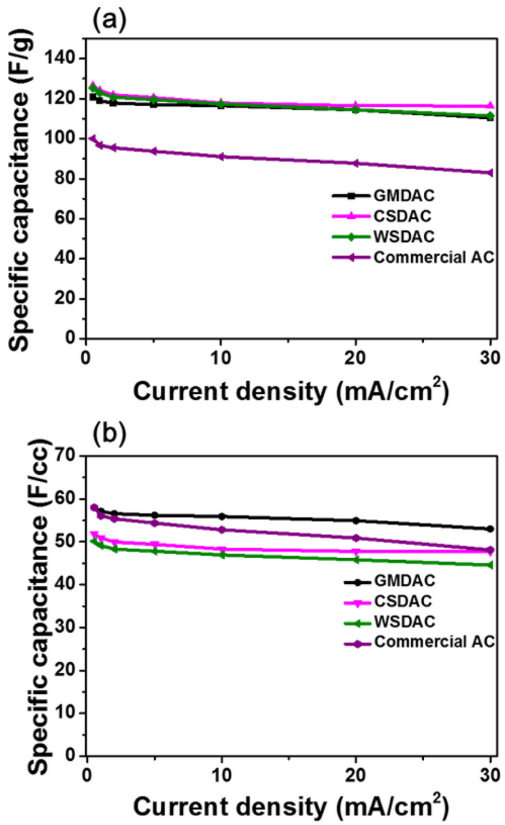

Fig. 5. (a) Gravimetric specific capacitance and (b) volumetric specific capacitance of GMDAC, CSDAC, WSDAC, and commercial AC measured at various current densities.

area compared to those of the other samples. However, the volumetric specific capacitances of all the samples are the same or lower compared to those of commercial AC due to their lower electrode densities (GMDAC: 0.48 g/cc, CSDAC: 0.41 g/cc, WSDAC: 0.40 g/cc, and commercial AC: 0.58 g/cc).

4. Conclusions

In the study, abundant agricultural waste-derived activated carbons were prepared to determine their commercial viability. The results reveal that commercially valuable activated carbons with specific surface areas exceeding 2000 m^2/g were successfully prepared from giant miscanthus, corn stalk, and wheat stalk by KOH activation. With respect to the herbaceous biomass-derived activated carbons, CSDAC exhibited the highest specific surface area, gravimetric specific capacitance (127 F/g), and capacitance retention ratio (92% at 30 mA/cm^2) due to its bimodal pore structure. On the other hand, GMDAC displayed the highest volumetric specific capacitance due to its relatively higher electrode density compared to that of the other samples. Thus, all the herbaceous biomass waste-derived activated carbons are potential energy storage materials in terms of economy and environment.

Acknowledgment

The study received support from the "R&D Program for Forest Science Technology (Project No. 2017053B10-1819-BB02)" of Korea Forest Service (Korea Forestry Promotion Institute).

This work was carried out with the support of "Cooperative Research Program for Agriculture Science and Technology Development (Project No. PJ01382902)" Rural Development Administration, Republic of Korea.

References

[1] Chen. L, et al., *J. Mater. Chem.* A, **2014**, *2(25),* 9684-9690.
[2] Basta. A, Fierro. V, El-Saied. H, Celzard. A, *Bioresour. technol,* **2009**, *100(17)*, 3941-3947.
[3] Wang. R, Wang. P, Yan. X, Lang. J, Peng. C, Xue. Q, *ACS appl. mater. Interfaces,* **2012**, *4(11)*, 5800-5806.
[4] Daifullah. A, Yakout. S, Elreefy. S, *J. Hazard. Mater,* **2007**, *147(1-2)*, 633-643.
[5] Hong. J, Hwang. B, Lee. J, Kim. K, *J. Electrochem. Sci. Technol*, **2017**, *8(1)*, 1-6.
[6] Kim. J, Chun. J, Kim. S-G, Ahn. H, Roh, K. C, *J. Electrochem. Sci. Technol*, **2017**, *8(4)*, 338-343.
[7] Yoo. J, Kim. Y, Lee. C-W, Yoon. H, Yoo. S, Jeong. H, *J. Electrochem. Sci. Technol*, **2017**, *8(3)*, 250-256.
[8] Kim. D, Rhee. K, Park. S, *J. Alloys Compd,* **2012**, *530*, 6-10.
[9] Zhang. S, Li. Y, Pan. N, *J. Power Sources,* **2012**, *206*, 476-482.
[10] Zou. J., et al., *Bioresour. Technol,* **2013**, *142*, 209-217.
[11] Saka. C, *J. Anal. Appl. Pyrolysis, **2012**, 95, 21-24.*
[12] Kim. S-I, et al, *Microporous and Mesoporous Materials,* **2006**, *96(1)*, 191-196.
[13] Bo. Li, Hiroshi. S, Hailong. J, Xinbo. Z, Qiang. X, *Carbon*, **2010**, *48*, 456-463.
[14] Chmiola. J, Yushin. G, Gogotsi. Y, Portet. C, Simon. P, Taberna. P. L, *Science,* **2006**, *313(5794)*, 1760-1763.
[15] Fan. Z, Yan. J, Wei. T, Zhi. L, Ning. G, Li. T, Wei. F, *Adv. Funct. Mater,* **2011**, *21(12)*, 2366-2375.
[16] Largeot. C, Portet. C, Chmiola,. J, Taberna. P-L, Gogotsi. Y, Simon. P, *J. Am. Chem. Soc,* **2008**, *130(9)*, 2730-2731.
[17] Rodriguez-Martinez, L. M, Omar. N., *Emerging Nanotechnologies in Rechargeable Energy Storage Systems. Elsevier Science,* **2017**.